Special Issue of the 6th International Congress & Exhibition (APMAS2016), Maslak, Istanbul, Turkey, June 1–3, 2016

New Kinetic Theory for Absorption and Emission Rates of Radiation and New Equations for Lattice and Electronic Heat Capacities, Enthalpies and Entropies of Solids: Application to Copper

A.E. Bozdoğan*

Yıldız Technical University, Department of Chemistry, Davutpaşa, 34220, Esenler, Istanbul, Turkey

New equations, which have analytical solutions, for lattice and electronic heat capacities, entropies and enthalpies at constant volume and constant pressure were derived by using kinetic theory, Kirchhoff and Stefan-Boltzmann laws and Wien radiation density equation. These equations were applied to the experimental constant volume heat capacity data of copper. The temperature Θ_V corresponding to $3R/2$ was found to be 78.4 K for copper. Copper shows the dimensionality crossover from 3 to 2 at about 80 K. The $\Theta_V(T)$ is proportional to Debye temperature. The relationship between dimension and Θ_V was given. Temperature dependence of Debye temperature and non-monotonic behavior were discussed. The heat capacity and entropy values, predicted by the proposed models were compared with the values predicted by the Debye models. The results have shown that the proposed models fit the data better than the Debye models. Enthalpy equations derived in this study were compared with the polynomial model and a good fitting was obtained. The equation for the photon absorption equilibrium constant of copper was derived.

DOI: 10.12693/APhysPolA.131.519

PACS/topics: 44.40.+a, 65.40.Ba, 65.40.Gr

1. Introduction

Heat capacity is the fundamental quantity for calculating thermodynamic functions like enthalpies, entropies and Gibbs free energies of solids. Different analytical models have been proposed in the past for analytical description of heat capacities. Einstein's single oscillator model is the first quantum statistical model for the temperature dependences of heat capacities of solids [1]. This model could not satisfactorily describe the experimentally obtained temperature dependences of heat capacities at low temperatures [2–4].

Nernst and Lindemann's two-oscillator model in comparison with Einstein's model have made the improvements of fitting of heat capacity data over large temperature regions. In this model, the ratio for the respective oscillation frequencies was taken to be 1/2. However, this model could not well describe the heat capacities in the cryogenic region $T < 100$ K [5].

Einstein and Nernst-Lindemann models have used the discrete oscillation frequencies, and the resulting theoretical curves, obtained by these models, show a plateau behavior in the $T \to 0$ K limit. In Debye model, atomic system is considered to be a three dimensional, elastic, isotropic continuum, and the single Einstein frequency is replaced by a frequency distribution function $a\omega^2$ [6]. Debye frequency function is a parabola open upward over the range from 0 to the Debye limiting frequency ω_D. The temperature corresponding to the Debye frequency ω_D is called the Debye temperature Θ_D. The heat capacity is given by [2–4, 6, 7]:

$$C_V = 9R\left(\frac{T}{\Theta_D(T)}\right)^3 \int_0^{x_\mathrm{D}} \frac{x^4 \mathrm{e}^x}{\left(\mathrm{e}^x - 1\right)^2}\,\mathrm{d}x, \tag{1}$$

where $x = \Theta_D(T)/T$ and R is the gas constant. The Debye temperature $\Theta_D(T)$ is given by [7]:

$$\Theta_D(T) = \frac{h}{k_\mathrm{B}}\left(\frac{3N_\mathrm{A}}{4\pi V_m}\right)^{1/3} v, \tag{2}$$

where h is the Planck constant, k_B is the Boltzmann constant, N_A is the Avogadro number, V_m is the molar volume of atom and v is the speed of sound. In the Debye model, heat propagates in the solid as sound waves. These waves are treated as energy particles called phonons, traveling at speeds, having two transverse and one longitudinal velocities [4]. v is given by [3]:

$$\frac{3}{v^3} = \frac{1}{v_\mathrm{l}^3} + \frac{2}{v_\mathrm{t}^3}, \tag{3}$$

where v_l and v_t are the velocities of longitudinal and transverse acoustic waves in solid.

The entropy equation in the Debye model is given by [2, 3, 6]:

$$S = 3R\left[\frac{4}{x_\mathrm{D}^3}\int_0^{x_\mathrm{D}} \frac{x^3\,\mathrm{d}x}{\left(\mathrm{e}^x - 1\right)} - \ln\left(1 - \mathrm{e}^{-x_\mathrm{D}}\right)\right]. \tag{4}$$

The analytical solutions of integrals in Eqs. 1 and 4 are not known. Therefore, at the intermediate temperatures, the values of heat capacities and entropies must be obtained by numerical integration.

*e-mail: bozdogan@yildiz.edu.tr

At very low temperatures, where $T \ll \Theta_D$, the following equation is obtained from Eq. (1):

$$C_V \cong \frac{12\pi^4 R}{5}\left(\frac{T}{\Theta_D(T)}\right)^3. \quad (5)$$

Equation (5) is known as the Debye T^3-law and assumed to be valid from 0 K up to lattice temperatures of order of $\Theta_D(0)/50$, where $\Theta_D(0)$ is the Debye temperature at $T \to 0$ K. Generally, as the temperature is increased from 0 K, $\Theta_D(0)$ value remains practically constant up to about $T \approx \Theta_D(0)/50$. It then decreases, and after passing through a minimum at $T \approx \Theta_D(0)/10$ starts to increase to a constant plateau at about $T \approx \Theta_D(0)/2$, [2, 3, 8]. Therefore, it is often impossible to provide good fitting of Eq. (1) to the given heat capacity data set with a single Debye temperature over the entire temperature range [3, 8]. These non-Debye behaviors have been given in terms of C_V/T^3 functions [9–11]. These curves show a non-monotonic behavior in the low temperature region which cannot be explained with the Debye's model.

The departure from T^3-law in the temperature interval $\theta_D(0)/50 \le T \le \theta_D(0)/10$ was assumed to be due to the deviation of density of modes of a real solid from the assumed ω^2-distribution. At these temperatures, the following equation has been given by a Taylor series expansion of the form [3, 8, 12]:

$$C_v \cong \frac{12\pi^4 R}{5\Theta_D^3(0)}T^3 + c_5T^5 + c_7T^7 + \ldots, \quad (6)$$

where the terms T^5, T^7,..., are assumed to be responsible for the non-Debye behavior in the cryogenic region and the coefficients c^3, c^5, c^7, ..., cannot be related to the limiting Debye temperature. At high temperatures, the following equation is obtained from Eq. (1) [2, 3, 5]:

$$C_V \cong 3R\left[1 - \frac{1}{20}\left(\frac{\Theta_D(\infty)}{T}\right)^2 + \ldots\right], \quad (7),$$

where $\Theta_D(\infty)$ is the Debye temperature at $T \to \infty$ K.

Different models based on Thirring and exponential series expansions have also been given for the intermediate to high temperature regions, respectively [5]. However, these models are complex and sets of seven or eight empirical parameters should be determined.

The heat capacity of a free electron gas in three dimensions for $T \ll T_F$ has been given by [7]:

$$C_{el} = 3R\frac{\pi^2}{6}\frac{T}{T_F}, \quad (8)$$

where T_F is the Fermi temperature. For high temperatures, the following equation has been given in [3]:

$$C_{el} = \frac{3}{2}Rz\left[1 - \frac{1}{6(2\pi)^{3/2}}\left(\frac{T_F}{T}\right)^{3/2}\ldots\right], \quad (9)$$

where z is the number of free electrons per atom. For intermediate values of (T/T_F), C_{el} must be computed numerically.

The analytical solutions of heat capacity and entropy equations given by Debye are not known. Therefore, at the intermediate temperatures, the values of heat capacities and entropies must be obtained by numerical integration. Lattice heat capacity at constant pressure, lattice molar enthalpy, electronic molar enthalpy and entropy equations have not been given in the past. The temperature dependence of Debye temperature and deviation from monotonicity have not been explained. In order to solve these problems, new kinetic theory for radiation and new equations will be proposed. These equations will be applied to the heat capacity data of copper and the results will be compared with the results obtained by Debye equations.

2. Theoretical

2.1. Heat capacity equations

Kirchhoff had proposed that, at equilibrium, any two different areas on the interior wall of a thermostated chamber of any geometry must emit and absorb radiation at equal rates to maintain equilibrium. If the emissivity of radiant energy, emitted from an element into the chamber is e and the fraction of radiant energy absorbed from incident radiation of intensity $I(\lambda, T)$ is a, the energy absorbed is $aI(\lambda, T)$. The energy absorbed must be equal to the energy emitted e for the condition of thermal equilibrium to be satisfied [4]:

$$aI(\lambda, T) = e. \quad (10)$$

The intensity is a function of only λ and T for cavity radiation, because e and a are functions of λ and T:

$$a(\lambda, T)\, I(\lambda T) = e(\lambda T). \quad (11)$$

This is the Kirchhoff's law. The intensity of radiation is related to the energy density:

$$I(\lambda, T) = \frac{c}{4\pi}u(\lambda T), \quad (12)$$

where $u(\lambda T)$ is the energy density and c is the speed of electromagnetic radiation in vacuum. Because of the reciprocal relationship between wavelength and frequency of electromagnetic radiation, the notations $I(\lambda T)$, $I(\nu T)$ and $u(\lambda, T), u(\nu T)$ are equivalent.

Stefan-Boltzmann radiation law had shown that the radiation density $u(T)$ for three degrees of freedom, three dimensions, within a blackbody cavity is given as follows [4]:

$$u(T) = 3p = \frac{8\pi^5 k_B^4}{15h^3c^3}T^4 = \beta T^4, \quad (13)$$

where p is the radiation (photon) pressure. From Eq. (12), the following equation can be written:

$$I(T) = \frac{c}{4\pi}u(T), \quad (14)$$

where $I(T) = \int_0^\infty I(\lambda, T)\, d\lambda$ and $u(T) = \int_0^\infty u(\lambda, T)\, d\lambda$. Substituting Eq. (13) into Eq. (14) gives:

$$I(T) = \frac{3c}{4\pi}p \quad (15)$$

From Eq. (11), the following equation can be written:

$$a(T)\, I(T) = e(T), \quad (16)$$

where $a(T) = \int_0^\infty a(\lambda, T)\, d\lambda$ and $e(T) = \int_0^\infty e(\lambda, T)\, d\lambda$. Substitution of Eq. (15) into Eq. (16) gives:

$$a(T)\frac{3c}{4\pi}p = e(T). \tag{17}$$

Equation (17) shows that the energy absorbed per unit area in unit time depends on the photon pressure p and $a(T)$.

The total phonon energy of a solid, given by Debye for three dimensions at temperature T is [4, 7]:

$$U(T) = \frac{9Nk_{\mathrm{B}}T^4}{\Theta_{\mathrm{D}}^3(T)}\int_0^{x_{\mathrm{D}}}\frac{x^3}{\mathrm{e}^x-1}\,\mathrm{d}x. \tag{18}$$

At low temperatures, Eq. (18) becomes:

$$U(T) = \frac{3\pi^4 Nk_{\mathrm{B}}}{5\Theta_{\mathrm{D}}^3(T)}T^4, \tag{19}$$

where N is the number of atoms in the solid. The T^4 variation of the phonon energy, given by Eq. (19) is the acoustic equivalent of the Stefan-Boltzmann law [2, 3]. The acoustic equivalent of the Stefan-Boltzmann law in units of Joule per mole can be written from Eq. (13) as:

$$U(T) = \frac{4\pi^5 k_{\mathrm{B}}^4 V_m}{5h^3v^3}T^4 = \frac{3V_m c^3}{2v^3}3p. \tag{20}$$

The factor $3/2$ accounts for the fact that phonons travelling at speed have two transverse and one longitudinal amplitude. From Eq. (19) and Eq. (20), the following equation can be written:

$$U(T) = \frac{3\pi^4 N_{\mathrm{A}}k_{\mathrm{B}}}{5\Theta_{\mathrm{D}}^3(T)}T^4 = \frac{4\pi^5 k_{\mathrm{B}}^4 V_m}{5h^3v^3}T^4 = \frac{3V_m c^3}{2v^3}3p. \tag{21}$$

Equation (2) can be obtained from Eq. (21). Equation (21) shows that the phonon energy (energy absorbed) depends on the photon pressure, as given in Eq. (17).

A calorimeter containing any solid at thermal equilibrium at any temperature above 0 K contains energy particles (photons). After thermal equilibrium has been established within a calorimeter at some temperature ($T > 0$ K), constant temperature within the calorimeter shows that the solid must be absorbing and emitting photons at the same rate. The equilibrium number of photons within the calorimeter is determined only by the temperature. The photons can be created or destroyed by changing the temperature of the calorimeter [4].

In the system of solid and photons, in a calorimeter, at any temperature ($T > 0$ K), the photons will be striking the solid and a fraction of photons will be absorbed. After thermal equilibrium has been established within the calorimeter at some temperature ($T > 0$ K), the rate at which photons strike the solid will be exactly balanced by the rate at which photons leave the solid.

The rate of absorption r_a will be equal to the rate of collisions r_c of photons with the solid, multiplied by a factor δ representing the fraction of the colliding photons that are absorbed. At a constant temperature ($T > 0$ K), the number of collisions will be proportional to the photon pressure p and the fraction δ will be constant. The rate of absorption will be $r_c\delta$. This is equal to $k_{\mathrm{a}}p$, where k_{a} is a constant involving the fraction δ and the proportionality between r_c and p.

Since the absorption is limited to the total number of electrons and atoms (particles) N_{t} in the solid, these particles may be divided into two groups. N is the number of photon absorbed particles and $(N_{\mathrm{t}} - N)$ is the number of photon unabsorbed particles. Since only those, photons, which are striking the unabsorbed particles, can be absorbed, the rate of absorption will be proportional to $(N_{\mathrm{t}} - N)$:

$$r_a = k_{\mathrm{a}}p\,(N_{\mathrm{t}} - N)\,. \tag{22}$$

The rate of emission will be proportional to the number of photon absorbed particles:

$$r_{\mathrm{e}} = k_e N. \tag{23}$$

At thermal equilibrium at any temperature ($T > 0$ K), the rate of absorption will be equal to the rate of emission:

$$k_{\mathrm{a}}p(N_{\mathrm{t}} - N) = k_e N. \tag{24}$$

Equation (24) is comparable with Eq. (17). Stefan-Boltzmann law is given as [4]:

$$p = \frac{T}{4}\frac{\mathrm{d}p}{\mathrm{d}T}. \tag{25}$$

Substituting Eq. (25) into Eq. (24) gives:

$$k_{\mathrm{a}}(N_{\mathrm{t}} - N)\frac{\mathrm{d}p}{\mathrm{d}T} = \frac{4}{T}k_e N. \tag{26}$$

If the temperature dependences of V_m and v are neglected, the following equations are obtained from Eq. (21):

$$\left(\frac{\partial U(T)}{\partial T}\right)_V = C_V = \frac{9V_m c^3}{2v^3}\frac{\mathrm{d}p}{\mathrm{d}T}, \tag{27}$$

$$\left(\frac{\partial U(T)}{\partial T}\right)_V = \frac{12\pi^4 N_{\mathrm{A}}k_{\mathrm{B}}T^3}{5\Theta_{\mathrm{D}}^3(T)} = \frac{16\pi^5 k_{\mathrm{B}}^4 V_m T^3}{5h^3v^3}. \tag{28}$$

Substituting Eq. (27) and Eq. (28) into Eq. (26) gives:

$$\frac{N}{N_{\mathrm{t}}} = \frac{C_V}{C_V + C_V'} = \frac{T^3}{T^3 + \Theta_V^3(T)}, \tag{29}$$

$$C_V' = \frac{18c^3V_m}{v^3KT}, \tag{30}$$

$$\Theta_V^3(T) = \frac{15c^3V_m\Theta_{\mathrm{D}}^3(T)}{2\pi^4N_{\mathrm{A}}k_{\mathrm{B}}v^3KT} = \frac{45h^3c^3}{8\pi^5k_{\mathrm{B}}^4KT}, \tag{31}$$

where $K = k_{\mathrm{a}}/k_{\mathrm{e}}$ is the photon absorption equilibrium constant. From Eq. (29), when $T \to \infty$,

$$C_V + C_V' = 3R, \tag{32}$$

From Eqs. (29) and (32), the following equation can be written for three dimensions:

$$C_V = 3R\frac{T^3}{T^3 + \Theta_V^3(T)}, \tag{33}$$

where $\Theta_V(T)$ is the temperature at $C_V = 3R/2$. At low temperature, the following equation can be written:

$$C_V = 3R\left(\frac{T}{\Theta_V(T)}\right)^3. \tag{34}$$

From Eqs. (5) and (34), the following equation is obtained:

$$\Theta_V(T) = \Theta_{\mathrm{D}}(T)\left(\frac{5}{4\pi^4}\right)^{1/3}. \tag{35}$$

DeSorbo has predicted that one dimensional solid has $C_V \propto T$ at low temperatures [13]. Benedict et al. have predicted that a two-dimensional graphite sheet has $C_V \propto T^2$ and $C_{\mathrm{el}} \propto T^2$, a one dimensional single-walled carbon nanotube has $C_V \propto T$ and $C_{\mathrm{el}} \propto T$, bulk graphite has $C_V \propto T^{2-3}$, and multi-walled tubes show a range of behavior intermediate between $C_V \propto T$ and $C_V \propto T^{2-3}$, at low temperatures [14]. De Heer has shown that graphite has $C_V \propto T^3$ and a three dimensional character from 0 to 150 K, and has $C_V \propto T^2$ and a two dimensional character above 150 K [15]. Hone et al. have shown experimentally that single-walled carbon nanotubes represent $C_V \propto T$ and one dimensional character at low temperature, and represent $C_V \propto T^2$ and a two dimensional character at higher temperatures, and the bundles of single-walled carbon nanotubes represent $C_V \propto T^3$ and a three dimensional character at low temperatures [16]. These results show that the heat capacity changes as a power of the temperature $C_V \propto T^{1-3}$, depending on dimension and temperature.

Wien has proposed the following equation for the total radiation density at all frequencies [4]:

$$u(T) = \frac{\alpha n!}{\left(\frac{\beta'}{T}\right)^{n+1}}, \tag{36}$$

where $\alpha = ac^{\gamma+1}$, $n = -(\gamma+2)$, $\beta' = b/c$, c is the speed of electromagnetic radiation in vacuum, a and b are constants. If $n = 3$ is used in Eq. (36), the following equation is obtained:

$$u(T)_3 = \frac{6a}{b^4}T^4 = \beta T^4. \tag{37}$$

This is Stefan's law which has been derived for three degrees of freedom and three dimensions. If the parameter n in Eq. (36) is assumed to be equal to dimension, then, the following equations can be derived from Eq. (36) for $n = 2$ and $n = 1$, respectively:

$$u(T)_2 = \frac{b}{3}\beta T^3, \tag{38}$$

$$u(T)_1 = \frac{b^2}{6}\beta T^2. \tag{39}$$

Equations (37–39) can also be derived, if the Stefan's law is written as follows:

$$u(T)_n = np = T\frac{\mathrm{d}p}{\mathrm{d}T} - p. \tag{40}$$

From Eqs. (37–39), the following equation can be written:

$$u\,(T)_n = np = (\mathrm{const})_n T^{n+1}. \tag{41}$$

From Eq. (21) and Eq. (37), the following equation can be written:

$$U\,(T) = \frac{3V_m c^2}{2v^3}u(T)_3. \tag{42}$$

Similar equations can be written for $u(T)_2$ and $u(T)_1$. For n dimensions, the following relation can be written:

$$U(T)_n \propto u(T)_n. \tag{43}$$

From Eq. (40), the following equation can be written:

$$p = \frac{T}{n+1}\frac{\mathrm{d}p}{\mathrm{d}T}. \tag{44}$$

Substitution of Eq. (44) into Eq. (26) gives:

$$k_{\mathrm{a}}(N_{\mathrm{t}} - N)\frac{\mathrm{d}p}{\mathrm{d}T} = \frac{n+1}{T}k_e N. \tag{45}$$

From Eq. (41) and Eq. (43), the following equation can be written:

$$\left(\frac{\partial U(T)}{\partial T}\right)_V = C_V \propto \frac{\mathrm{d}p}{\mathrm{d}T} \propto T^n. \tag{46}$$

Substitution of Eq. (46) into Eq. (45) gives:

$$\frac{N}{N_{\mathrm{t}}} = \frac{C_V}{3R} = \frac{T^n}{T^n + \Theta_V^n(T)}. \tag{47}$$

At low temperature, the following equation can be written:

$$C_V = 3R\left(\frac{T}{\Theta_V(T)}\right)^n. \tag{48}$$

Equation (48) agrees with the relation given above $C_V \propto T^{1-3} \propto T^n$.

Similar equation can be written for the heat capacity at constant pressure C_P:

$$C_P = C_{P\max}\frac{T^n}{T^n + \Theta_p^n(T)}, \tag{49}$$

where $C_{P\max}$ is the heat capacity at $T \to \infty$, $\Theta_P(T)$ is the temperature at $C_{P\max}/2$. $C_{P\max}$ was not known before and can be predicted from Eq. (49). For $n = 3$, the following equation can be written:

$$C_P = C_{P\max}\frac{T^3}{T^3 + \Theta_p^3(T)}. \tag{50}$$

For the electronic heat capacity, the following equation can be written:

$$C_{\mathrm{el}} = \frac{3}{2}R\frac{T^n}{T^n + T_{\mathrm{E}}^n(T)}, \tag{51}$$

where $T_{\mathrm{E}}(T)$ is the temperature at $C_{\mathrm{el}} = 3R/4$. If $n = 1$ and $T \ll T_{\mathrm{E}}$, the following equation can be written from Eq. (51):

$$C_{\mathrm{el}} = \frac{3}{2}R\frac{T}{T_{\mathrm{E}}(T)}. \tag{52}$$

From Eq. (8) and Eq. (52), the following equation is obtained:

$$T_{\mathrm{E}} = \frac{3}{\pi^2}T_{\mathrm{F}}. \tag{53}$$

At low temperatures, the heat capacity of solids may be written as the sum of electronic and lattice heat capacities:

$$C_V = \gamma T + AT^3, \tag{54}$$

where γ and A are characteristic constants of the solid [7]. A plot of C_V/T versus T^2 should be a straight line with slope A and intercept γ. These plots allow both the determination of the Debye temperature $\Theta_{\mathrm{D}}(0)$ through $A = 12\pi^4 Rs/5\Theta_{\mathrm{D}}^3(0)$ and the observed value of the Fermi temperature through $\gamma = \pi^2 RT/2T_{\mathrm{F}}$.

2.2. Entropy equations

The absolute entropy is given by [2–4]:

$$S = \int_0^T \left(\frac{C}{T}\right)\mathrm{d}T. \tag{55}$$

Substitution of Eq. (51) into Eq. (55) and integration give the electronic molar entropy:

$$S_{\mathrm{el},n} = \frac{3}{2n} R \ln\left(\left(\frac{T}{T_{\mathrm{E}}(T)}\right)^n + 1\right). \tag{56}$$

Substitution of Eq. (47) into Eq. (55) and integration give the lattice molar entropy at constant volume:

$$S_{V,n} = \frac{3}{n} R \ln\left(\left(\frac{T}{\Theta_V(T)}\right)^n + 1\right). \tag{57}$$

For $n = 3$, the following equation is obtained from Eq. (57):

$$S_{V,n=3} = R \ln\left(\left(\frac{T}{\Theta_V(T)}\right)^3 + 1\right). \tag{58}$$

Equation (58) is comparable with Eq. (4) given by Debye. Substitution of Eq. (49) into Eq. (55) and integration give the lattice molar entropy at constant pressure:

$$S_{P,n} = \frac{C_{P\max}}{n} \ln\left(\left(\frac{T}{\Theta_P(T)}\right)^n + 1\right). \tag{59}$$

2.3. Enthalpy equations

The absolute enthalpy is given by [2, 3]:

$$H = \int_0^T C_P \,\mathrm{d}T. \tag{60}$$

Substitution of Eq. (49) into Eq. (60) gives:

$$H_{p,n} = C_{P\max} \int_0^T \frac{T^n}{\Theta_P^n(T) + T^n} \,\mathrm{d}T. \tag{61}$$

The integral in Eq. (61) can only be solved for $n = 1$, $n = 2$ and $n = 3$. This shows that n is related to the dimension. From Eq. (61), the lattice molar enthalpy equations at constant pressure are obtained for $n = 1$, $n = 2$ and $n = 3$:

$$H_{p,n=1} = C_{P\max}\left[T + \Theta_P \ln\left(\frac{\Theta_P}{T + \Theta_P}\right)\right], \tag{62}$$

$$H_{p,n=2} = C_{P\max}\left[T - \Theta_P \tan^{-1}\left(\frac{T}{\Theta_P}\right)\right], \tag{63}$$

$$H_{p,n=3} = C_{P\max}\left[-\frac{\pi}{6\sqrt{3}}\Theta_P + T - \frac{\Theta_P}{3}\ln\left(\Theta_P + T\right) + \frac{\Theta_P}{6}\ln\left(\Theta_P^2 - \Theta_P T + T^2\right) - \frac{\Theta_P}{\sqrt{3}}\tan^{-1}\left(\frac{2T - \Theta_P}{\sqrt{3}\Theta_P}\right)\right]. \tag{64}$$

If C_V is used instead of C_P in Eq. (61), the following equation can be written:

$$H_{V,n} = 3R \int_0^T \frac{T^n}{\Theta_V^n(T) + T^n} \,\mathrm{d}T. \tag{65}$$

From Eq. (65), the lattice molar enthalpy equations at constant volume are obtained for $n = 1$, $n = 2$ and $n = 3$.

$$H_{V,n=1} = 3R\left[T + \Theta_V \ln\left(\frac{\Theta_V}{T + \Theta_V}\right)\right], \tag{66}$$

$$H_{V,n=2} = 3R\left[T - \Theta_V \tan^{-1}\left(\frac{T}{\Theta_V}\right)\right], \tag{67}$$

$$H_{V,n=3} = 3R\left[-\frac{\pi}{6\sqrt{3}}\Theta_V + T - \frac{\Theta_V}{3}\ln\left(\Theta_V + T\right) + \frac{\Theta_V}{6}\ln\left(\Theta_V^2 - \Theta_V T + T^2\right) - \frac{\Theta_V}{\sqrt{3}}\tan^{-1}\left(\frac{2T - \Theta_V}{\sqrt{3}\Theta_V}\right)\right]. \tag{68}$$

If C_{el} is used instead of C_P in Eq. (61), the following equation can be written.

$$H_{\mathrm{el},n} = \frac{3}{2} R \int_0^T \frac{T^n}{T_{\mathrm{E}}^n(T) + T^n} \,\mathrm{d}T. \tag{69}$$

From Eq. (69), the electronic molar enthalpy equations are obtained for $n = 1$, $n = 2$ and $n = 3$.

$$H_{\mathrm{el},n=1} = \frac{3}{2} R\left[T + T_{\mathrm{E}} \ln\left(\frac{T_{\mathrm{E}}}{T + T_{\mathrm{E}}}\right)\right], \tag{70}$$

$$H_{\mathrm{el},n=2} = \frac{3}{2} R\left[T - T_{\mathrm{E}} \tan^{-1}\left(\frac{T}{T_{\mathrm{E}}}\right)\right], \tag{71}$$

$$H_{\mathrm{el},n=3} = \frac{3}{2} R\left[-\frac{\pi}{6\sqrt{3}}T_{\mathrm{E}} + T - \frac{T_{\mathrm{E}}}{3}\ln\left(T_{\mathrm{E}} + T\right) + \frac{T_{\mathrm{E}}}{6}\ln\left(T_{\mathrm{E}}^2 - T_{\mathrm{E}} T + T^2\right) - \frac{T_{\mathrm{E}}}{\sqrt{3}}\tan^{-1}\left(\frac{2T - T_{\mathrm{E}}}{\sqrt{3}T_{\mathrm{E}}}\right)\right]. \tag{72}$$

3. Results and discussion

Experimental heat capacity data at constant volume of copper for the temperature range from 1 K to 400 K were obtained from Ref. [17] and are shown in Fig. 1. The value of Θ_V was found to be 78.4 K. The value of $\Theta_{\mathrm{D}}(0)$ was found to be 344 K. Θ_{D} is found to be 334.8 K by using $\Theta_V = 78.4$ K in Eq. (35). The heat capacity values, calculated by using $\Theta_{\mathrm{D}} = 344$ K in Eq. (1) and the heat capacity values calculated by using $\Theta_V = 78.4$ K and $n = 3$ in Eq. (33) are also shown in Fig. 1.

The values of $\Theta_{\mathrm{D}}(T)$ were calculated from the numerical solution of Eq. (1). Temperature dependence of $\Theta_{\mathrm{D}}(T)$ of copper is shown in Fig. 2. It is seen from Fig. 2 that $\Theta_{\mathrm{D}}(T)$ increases monotonously from 138 K to the maximum 330 K with increasing temperature from 1 K to 12 K and passes through a broad maximum at about 12 K. It then decreases and passes through a minimum 310 K at about 35 K. It starts to increase towards 315 K at about 50 K.

By substituting Eq. (35) into Eq. (47), the following equation is obtained:

$$n = \frac{\log\left(\frac{3R}{C_V} - 1\right)}{\log\left(\Theta_{\mathrm{D}}\left(T\right)\left(5/4\pi^4\right)^{1/3}/T\right)}. \tag{73}$$

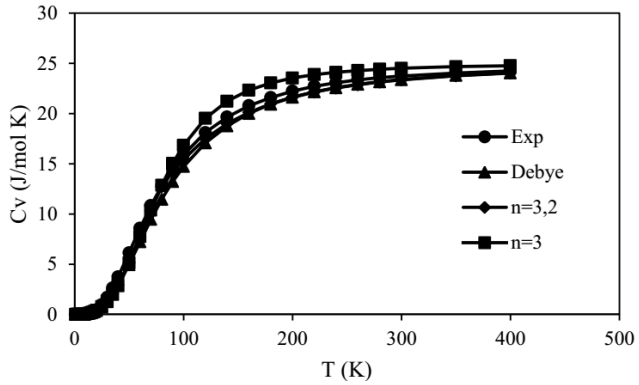

Fig. 1. Temperature dependence of heat capacity of copper.

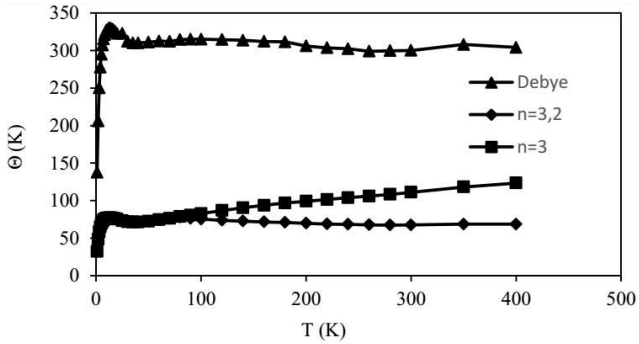

Fig. 2. Temperature dependence of $\Theta_{\mathrm{D}}(T)$ and $\Theta_V(T)$ of copper.

The temperature dependence of n of copper, obtained from $\Theta_{\mathrm{D}}(T)$ is shown in Fig. 3. It is seen from Fig. 3 that the value of n is about 3 from 1 K to 20 K. It then decreases and passes through a minimum 2.90 at about 40 K and then increases to 3 at 50 K. n exhibits a crossover from 3 to 2 at about 80 K. After 80 K, n takes a value of about 2. If the $\Theta_{\mathrm{D}}(T)$ is taken as a constant value of 330 K from 1 K to 12 K, n increases from 2.40 to 3.0 with increasing temperature from 1 K to 12 K. Figure 2 and Eq. (73) show that $\Theta_{\mathrm{D}}(T)$ depends on temperature and n.

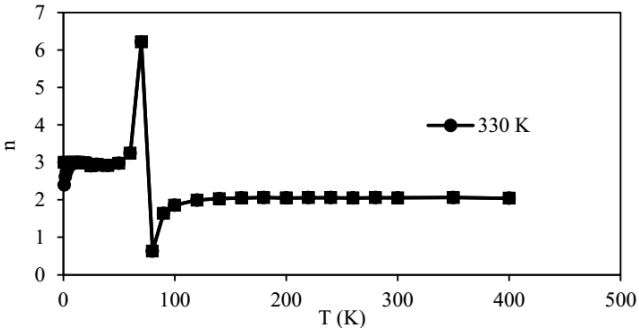

Fig. 3. Temperature dependence of n for copper.

The following equation is obtained from Eq. (47):

$$\Theta_V(T) = T\left(\frac{3R}{C_V} - 1\right)^{1/n}. \tag{74}$$

The values of $\Theta_V(T)$ were calculated by using $n = 3$ at all temperatures, and $n = 3$ from 1 K to 80 K and $n = 2$ from 80 K to 400 K in Eq. (74). Temperature dependence of $\Theta_V(T)$ is also shown in Fig. 2. It is seen from Fig. 2 that the temperature dependence of $\Theta_V(T)$ obtained by using $n = 3$ from 1 K to 80 K and $n = 2$ from 80 K to 400 K is similar to $\Theta_{\mathrm{D}}(T)$. But, $\Theta_V(T)$ obtained by using $n = 3$, is different at all temperatures.

The relationship between n and $\Theta_V(T)$ can be obtained from the first and second derivatives of Eq. (47):

$$\Theta_M(T) = \Theta_V(T)\left(\frac{n-1}{n+1}\right)^{1/n}, \tag{75}$$

where $\Theta_M(T)$ is the temperature corresponding to the inflexion point of the plot of Eq. (47) and exists if $n > 1$.

The non-monotonic behavior of the C_V/T^3 function at low temperatures is shown in Fig. 4. In this function, n is taken to be 3. According to Eq. (75), $\Theta_V(T)$ should change with temperature. The C_V/T^3 function is inversely proportional to $\Theta_V^3(T)$. Therefore, the C_V/T^3 function will show the inverse behavior to $\Theta_V^3(T)$.

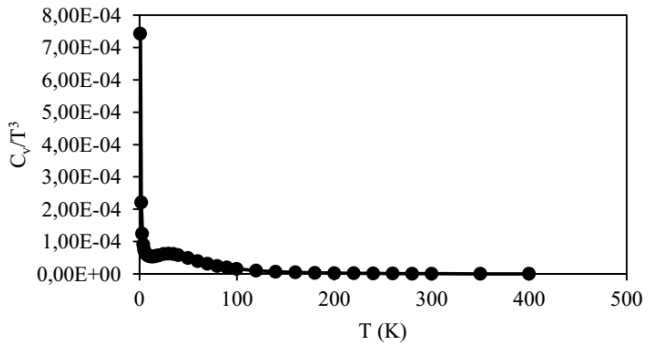

Fig. 4. C_V/T^3 versus T for copper.

In order to evaluate the predictive ability of the models, the root mean square error of prediction (RMSEP) is used:

$$\mathrm{RMSEP}(C_V) = \sqrt{\frac{\sum_{i=1}^{m}\left(C_{V\mathrm{pred}} - C_{V\mathrm{exp}}\right)^2}{m}}, \tag{76}$$

where $C_{V\mathrm{exp}}$ is the experimental heat capacity, $C_{V\mathrm{pred}}$ is the predicted heat capacity and m is the number of heat capacities. The value of RMSEP obtained for the proposed models by using $\Theta_V(T) = 78.4$ K and $n = 3$ from 1 K to 80 K and $n = 2$ from 80 K to 400 K was found to be 0.4302. The value of RMSEP obtained for the Debye model was found to be 0.6523. These results and Fig. 1 show that the proposed model obtained by using $n = 3$ from 1 K to 80 K and $n = 2$ from 80 K to 400 K fits the experimental data better than the other models. This result also shows that copper exhibits dimensionality crossover from 3 to 2 at about 80 K.

Temperature dependence of entropies obtained from the Debye, the proposed and the polynomial models are shown in Fig. 5.

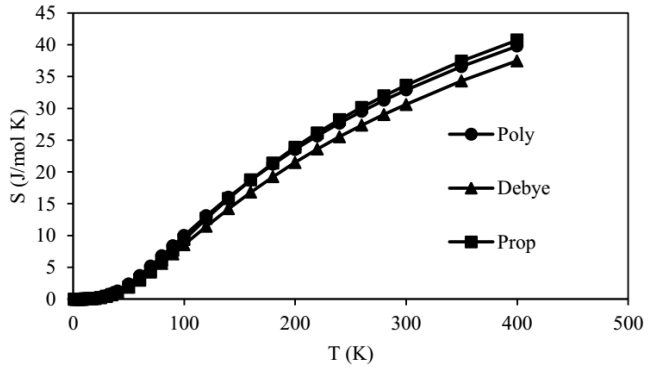

Fig. 5. Temperature dependence of entropy of copper.

The RMSEP is obtained from the following equation.

$$\mathrm{RMSEP}(S) = \sqrt{\frac{\sum_{i=1}^{m} (S_{\mathrm{pred}} - S_{\mathrm{poly}})^2}{m}}, \tag{77}$$

where S_{poly} is the entropy obtained from the polynomial model and S_{pred} is the entropy obtained from the proposed and the Debye models. The values of RMSEP obtained for the proposed and Debye models were found to be 0.4251 and 1.262, respectively. These results and Fig. 5 show that the proposed model fits the data better than the Debye model.

Enthalpy equation cannot be obtained from the Debye model. Temperature dependence of enthalpies obtained from the proposed and polynomial models are shown in Fig. 6.

The RMSEP is obtained from the following equation.

$$\mathrm{RMSEP}(H) = \sqrt{\frac{\sum_{i=1}^{m} (H_{\mathrm{pred}} - H_{\mathrm{poly}})^2}{m}}, \tag{78}$$

where H_{poly} is the enthalpy obtained from polynomial model and H_{pred} is the enthalpy obtained from the proposed model. The value of RMSEP was found to be 31.59. This result and Fig. 6 show that the proposed model fits the data very well.

If the temperature dependence of V_m and v are neglected, and $V_m = 7.116$ cm^3/mol, $v = 2612$ m/s at room temperature, $c = 3 \times 10^8$ m/s, $h = 6.626 \times 10^{-34}$ J s and $k_{\mathrm{B}} = 1.38 \times 10^{-23}$ J/K are used in Eqs. (30–32), the following equations are obtained for $n = 3$.

$$K = 1.94 \times 10^{11}/T(3R - C_V), \tag{79}$$

$$\Theta_V^3 = 2 \times 10^4 (3R - C_V). \tag{80}$$

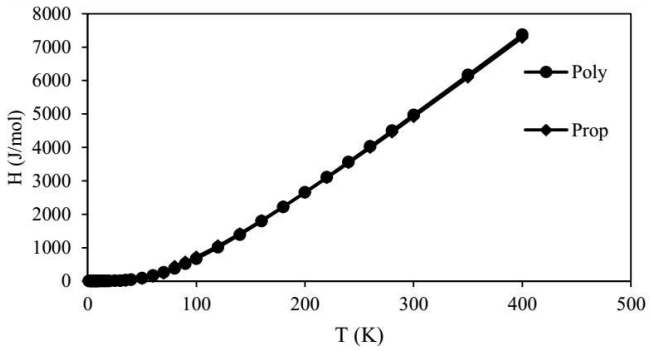

Fig. 6. Temperature dependence of enthalpy of copper.

4. Conclusions

New equations for lattice and electronic heat capacities, entropies and enthalpies at constant volume and constant pressure were derived and applied to the experimental constant volume heat capacity data of copper. The value of Θ_V was found to be 78.4 K for copper. Copper shows the dimensionality crossover from $n = 3$ to $n = 2$ at about 80 K. $\Theta_V(T)$ is proportional to $\Theta_{\mathrm{D}}(T)$. Temperature dependence of $\Theta_{\mathrm{D}}(T)$ and non-monotonic behavior were discussed. The relationship between n and $\Theta_V(T)$ was given. The root mean square error of prediction was used to compare the models. The heat capacity and entropy values predicted by the proposed model were compared with the values predicted by the Debye model. The results show that the proposed model fits the data better than the Debye model. Enthalpy equations cannot be obtained from the Debye model. The enthalpy equations derived in this study were compared with the polynomial model. The equation for the photon absorption equilibrium constant of copper was derived.

References

[1] A. Einstein, *Annals Phys.* **22**, 180 (1907).

[2] E.S.R. Gopal, *Specific Heats at Low Temperatures*, Plenum Press, New York 1966, p. 25.

[3] A. Tari, *The Specific Heat of Matter at Low Temperatures*, Imperial Collage Press, London 2003, p. 19.

[4] D.W. Rogers, *Einstein's Other Theory. The Planck-Bose Theory of Heat Capacity*, Princeton University Press, 2005, p. 33.

[5] R. Passler, *Phys. Status Solidi B* **245**, 1133 (2008).

[6] P. Debye, *Annals Phys.* **39**, 789 (1912).

[7] C. Kittel, *Introduction to Solid State Physics*, Wiley, New York 2005, p. 115.

[8] R. Passler, *Phys. Status Solidi B* **247**, 77 (2010).

[9] M. Sanati, S.K. Estreicher, M. Cardona, *Solid State Commun.* **131**, 229 (2004).

[10] A. Gibin, G.G. Devyathykh, A.V. Gusev, R.K. Kramer, M. Cardona, H.-J. Pohl, *Solid State Commun.* **133**, 569 (2005).

[11] M. Cardona, R.K. Kramer, M. Sanati, S.K. Estreicher, T.R. Antony, *Solid State Commun.* **133**, 465 (2005).

[12] P. Flubacher, A.J. Leadbetter, J.A. Morrison, *Phil. Mag.* **4**, 273 (1959).

[13] W. Desorbo, *J. Chem. Phys.* **21**, 1144 (1953).

[14] L.X. Benedict, S.G. Louie, M.L. Cohen, *Solid State Commun.* **100**, 177 (1996).

[15] W. de Heer, *Science* **289**, 1702 (2000).

[16] J. Hone, B. Battlogg, Z. Benes, A.T. Johnson, J.E. Fischer, *Science* **289**, 1730 (2000).

[17] G.K. White, S.J. Collocott, *J. Phys. Chem. Ref. Data* **13**, 1251 (1984).